Supporting Information

for

1,8-Naphthalimide based chemosensor for intracellular and in biofluid detection of Pd^{2+} ions: Microscopic and anticounterfeiting studies

Sanjeev Kumar[a], Neha Sharma[b], Satwinder Singh Marok[c], Satwinderjeet Kaur[b] and Prabhpreet Singh[a]*

[a]Department of Chemistry, UGC Centre for Advanced Studies-II, Guru Nanak Dev University, Amritsar 143001 (pb.)-India

[b]Department of Botanical and Environmental Sciences, Guru Nanak Dev University, Amritsar 143001 (pb.)-India

[c]Apotex Inc.,150 Signet Drive, Toronto, ON, M9L1T9 Canada

E-mail: prabhpreet.chem@gndu.ac.in; M: +91 8427101534.

*Synthesis of compound **1***

1,8-Naphthalic anhydride (20.2 mmol, 4.0 g) was dissolved in a 4M KOH solution (24 mL) and to this solution bromine (29.3 mmol, 1.55 mL) was slowly added. The mixture was stirred for 12 h at 65° C. After this time interval, the reaction mixture was cooled to room temperature and sulfuric acid (10 mL) was slowly added. The resulting solution was allowed to reflux for 1 h. The precipitates of 4-bromo-1,8-naphthalic anhydride were collected through filtration, washed with H_2O and methanol. The precipitates were dried (95% yield) and further used without purification. In the next step, 4-bromo-1,8-naphthalic anhydride (4.0 g, 14.0 mmol) and cyclohexylamine (1.72 g, 17.0 mmol) mixture was refluxed in ethanol (110 mL) for 12 h. The reaction mixture was cooled to room temperature and precipitates were collected by filtration, washed with ethanol and dried under vacuum to obtained compound **2**; Yield 57%; R_f = 0.63 chloroform: hexane (1:1); ^{1}H NMR (500 MHz, $CDCl_3$, 25 °C): δ 8.62 (dd, *J* = 7 Hz, 1H), 8.53 (dd, *J* = 8.5 Hz, 1H), 8.38 (d, *J* = 7.5 Hz, 1H), 8.02 (d, *J* = 8 Hz, 1H), 7.85-7.82 (m, 1H), 5.04-4.97 (m, 1H), 1.91-1.88 (m, 2H), 1.75-1.72 (m, 4H), 1.49-1.28 (m, 4H) ppm.

*Synthesis of **NPG***

To a solution of pentaethylene glycol (0.06 mL, 1.39 mol) in CH_3CN (25 mL), NaH (0.06 g, 1.39 mol) was added and the reaction mixture was stirred for 30 min at 70 °C under stream of N_2. Subsequently, compound **1** (0.5 g, 2.79 mol) was added to the above solution and reaction mixture was stirred for another 10 h at 70 °C. After completion of the reaction (tlc), the solvent was evaporated and water was added. The crude residue was extracted with CH_2Cl_2 (3x20 mL),

combined organic layers were dried over Na_2SO_4 and solvent was rotary evaporated. The crude residue was column chromatographed on silica (60–120 mesh) using $CHCl_3$–CH_3OH (90: 10, v/v) mixture as an eluent solution to obtained **NPG** as viscous liquid, Yield 35%, R_f = 0.18 (ethyl acetate); IR spectrum (ATR): ν_{max} [cm^-] = 3473.9, 2922.2, 2862.6, 2109.7, 1908.4, 1654.9, 1587.8, 1513.3, 1453.7, 1349.3, 1267.3, 1110.7, 939.3, 842.4, 752.9, 663.5, 521.8 and 454.7 cm^{-1}; ^{1}H NMR (500 MHz, $CDCl_3$, 25 °C): δ 8.48-8.56 (m, 3H), 7.68 (t, *J* = 7.5 Hz, 1H), 7.04 (d, *J* = 8 Hz, 1H), 5.01 (t, *J* = 12 Hz, 1H), 4.45 (s, 2H), 4.04 (s, 2H), 3.80 (s, 2H), 3.67 (d, *J* = 30.5 Hz, 12H) 3.87 (s, 2H), 1.90-1.72 (m, 6H), 1.48-1.31 (m, 4H) ppm; ^{13}C NMR (125 MHz, $CDCl_3$): δ 164.94, 164.38, 159.69, 133.20, 131.37, 129.39, 128.42, 125.88, 123.35, 122.99, 115.77, 106.09, 76.81, 72.64, 70.99, 70.57, 70.55, 70.50, 70.19, 69.42, 68.37, 61.65, 53.55, 29.67, 29.15, 26.60, 25.50. HR-MS: *m/z* found 515.228 (M^++H); calcd 515.603 (M^++H) for [$C_{28}H_{37}NO_8$].

Live cell imaging and MTT assay

For MTT assay, MG-63 (Human osteosarcoma) cell line was procured from the National Centre for Cell Science (NCCS) Pune, India. The cells were cultured in Dulbecco's modified Eagle's medium (DMEM) supplemented with an antibiotic–antimycotic solution and 10% fetal bovine serum (Biological Industries) by making a humidified atmosphere at 37^{o}C under 95% air mixture and 5% CO_2. The 1×PBS (pH 7.4) and trypsinized were used for the washing of the cells at 37^{0}C, followed by centrifugation at 1000 rpm for 5 min. The cytotoxic potential of **NPG** was determined by using an MTT assay. In this experiment, MG-63 cells were seeded in 96 well microplates at the concentration of 8x10^3 cells/0.1 ml and incubated to allow cell attachment. After 15h, cells were treated with the different concentrations of the **NPG** using serial dilutions method. On the completion of total 40h, 20 µl of 3-(4,5-dimethylthiazol-2-yl)-2,5-diphenyltetrazolium bromide (MTT) was added in each well and the ability of viable cells to reduce it into insoluble purple colored formazan was measured and the cells were further incubated for 3h. After this time, supernatant MTT solution was removed from each well and the intracellular MTT formazan was dissolved in 100 µl of dimethyl sulfoxide (DMSO). Finally, the decrease in absorbance was measured at 570 nm using a multi well plate reader (BioTek Synergy HT).

Cell viability = (Absorbance of treated sample/ Absorbance of untreated control) x 100

The growth inhibition percentage was expressed by using the following equation

% Growth inhibition = 100% viability.

Cells of two wells were treated with **NPG** (5 μM prepared in media with 2% DMSO); cells of 4 wells were treated with **NPG** (5 μM) for 30 minutes followed by addition of Pd^{2+} (2 wells each with 250 and 500 μM concentrations) and 2 wells served as control. For the cell imaging experiment, the MG-63 cells were seeded in a 24-well plate at a density of 3×10^5 cells/well and coverslip was placed in each well. After 24h, cells get adhered and then treated with various concentrations of **NPG**. After 30 minutes, media was discarded and cells were washed thrice with 1xPBS and on the slides, anti-fading reagent (Floromount, Sigma) was poured over the centre and then glass coverslip was gently put on it. Finally, the images were captured at excitation of 360 nm under a fluorescent Microscope system (Nikon Corporation, Japan) using NIS Elements AR analysis software version 4.11.00.

Limit of Detection

The limit of detection for Pd^{2+} ion was calculated based on the fluorescence titration. To determine the S/N ratio, the emission intensity of **NPG** (5 μM) solution (in triplicates) was determined and the standard deviation of blank solution (in the absence of analyte) measurements was determined. The detection limit was then considered using the equation, detection limit = 3σ/m, where σ the standard deviation of the blank solution (in the absence of analyte) measurements, and m is the slope between fluorescence intensity versus Pd^{2+} concentrations.

Preparation of TLC strips

TLC strips were prepared by dipping silica gel coated aluminium plate into the CH_3CN solution of **NPG**, followed by drying under vacuum at room temperature. The different concentrations of Pd^{2+} ions were prepared in DMSO solution and aliquot of 3 μL of each solution was added on the TLC strips previously coated with **NPG** (30 μM). For the control experiment, a drop of DMSO alone was also added on the TLC strip coated with **NPG**. These TLC strips were then visualized under 365 nm UV lamp.

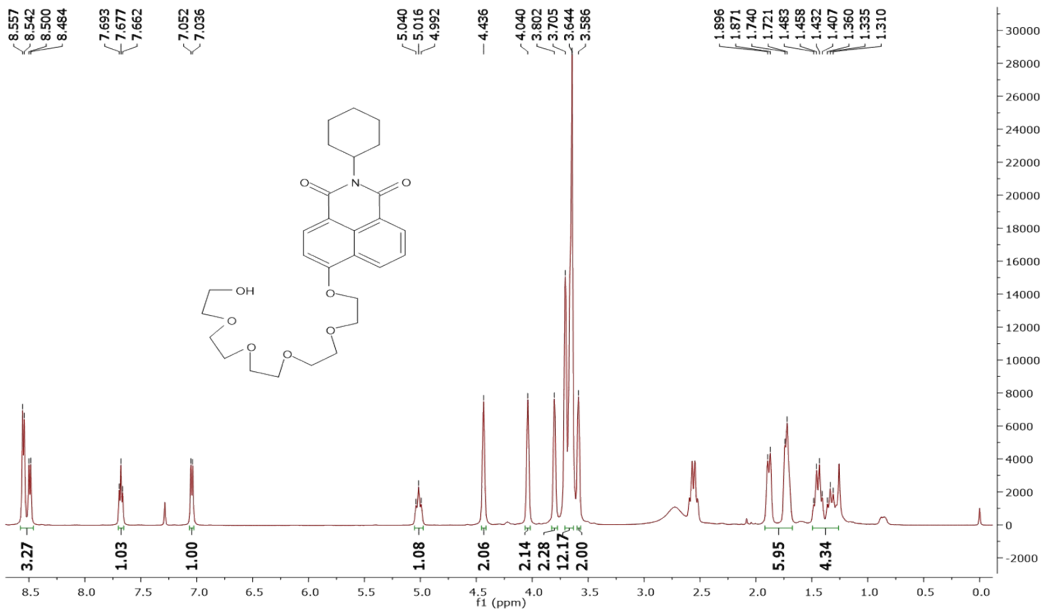

Figure S1a. ^{1}H NMR data of **NPG** in $CDCl_3$.

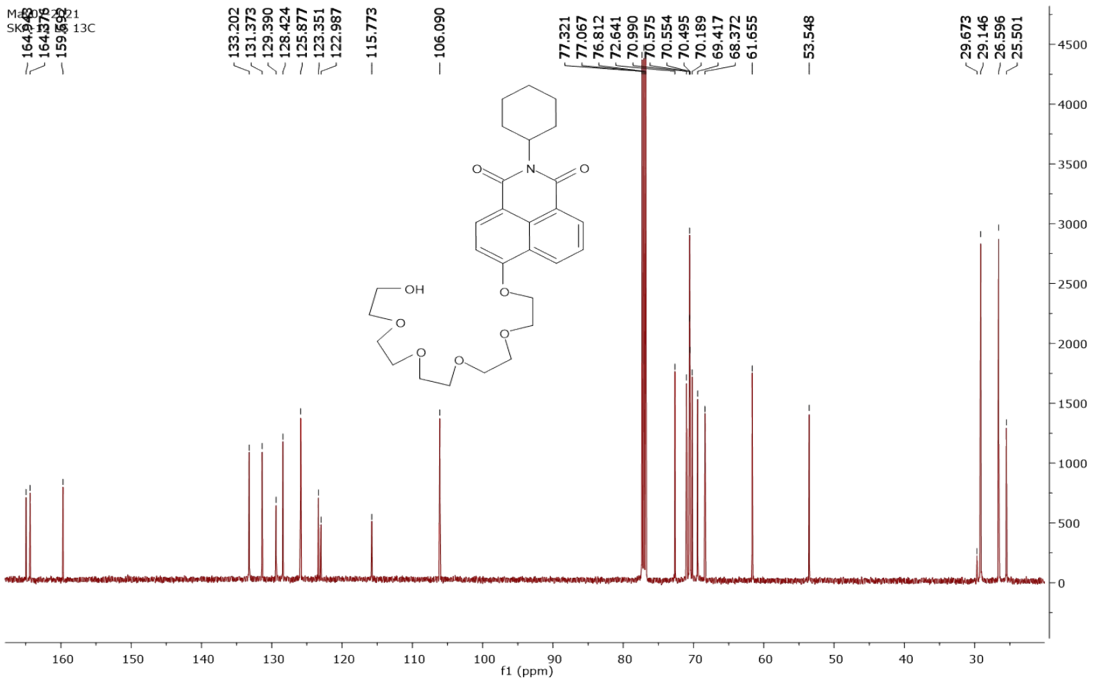

Figure S1b. ^{13}C NMR data of **NPG** in $CDCl_3$.

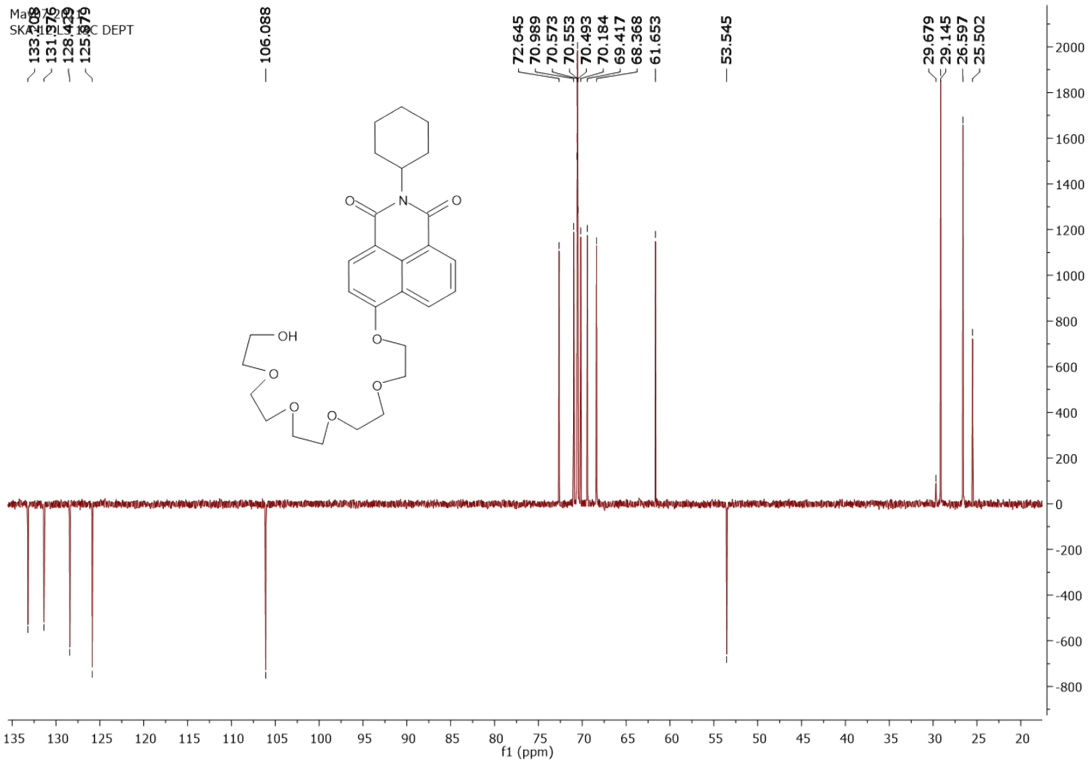

Figure S1c. ^{13}C DEPT-135 NMR data of **NPG** in $CDCl_3$.

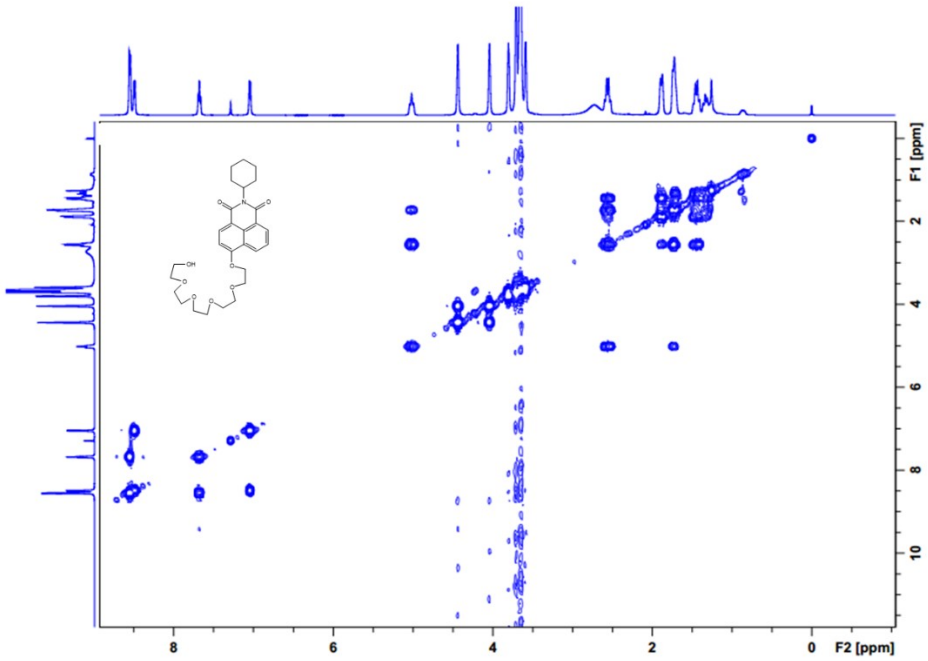

Figure S1d. ^{1}H-^{1}H cosy NMR data of **NPG** in $CDCl_3$.

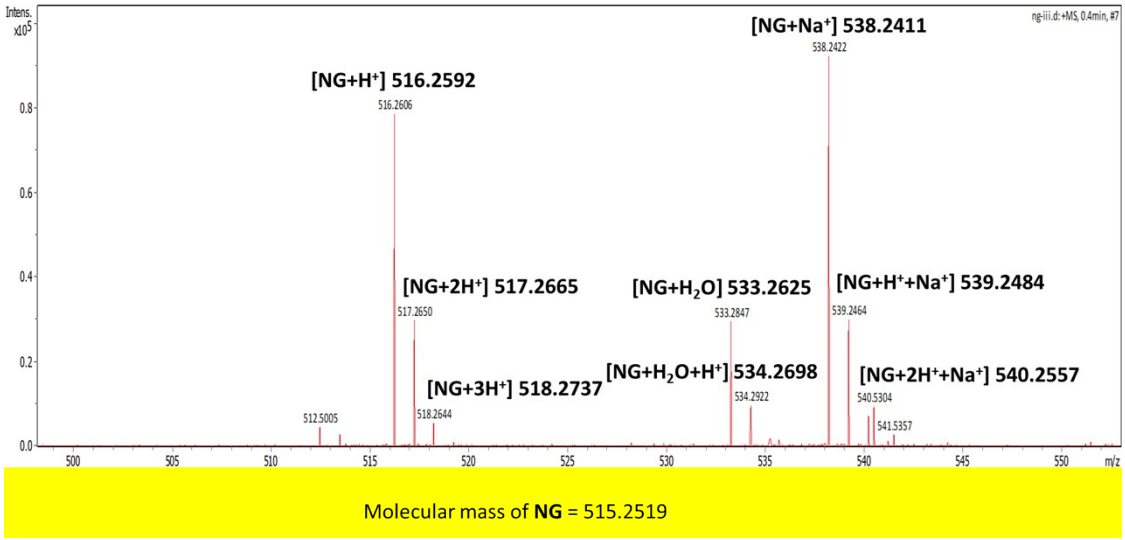

Figure S1e. HRMS-mass spectral data of **NPG**. NG=NPG in the figure caption

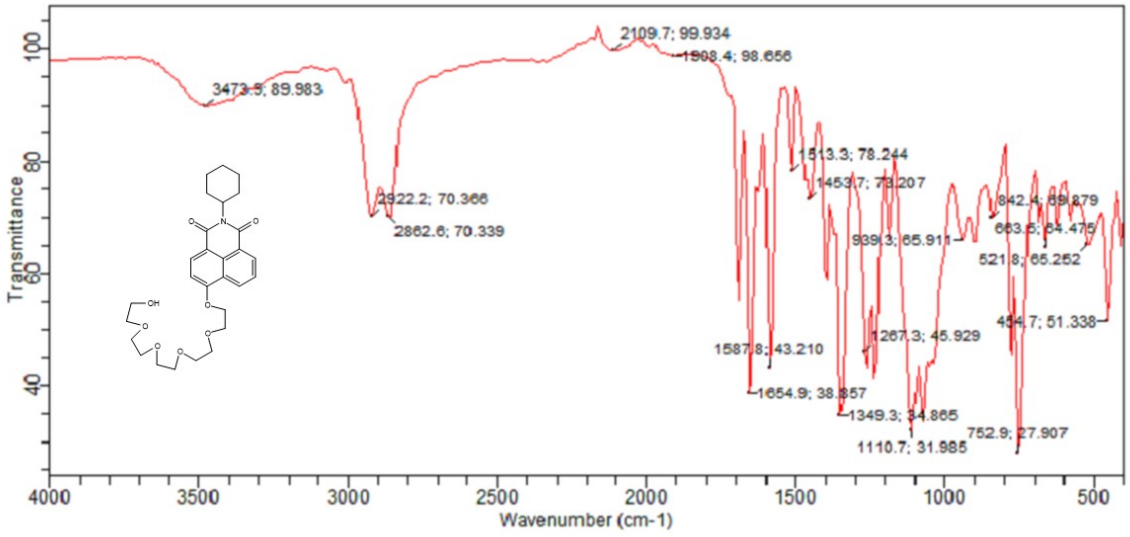

Figure S1f. FTIR data of **NPG**.

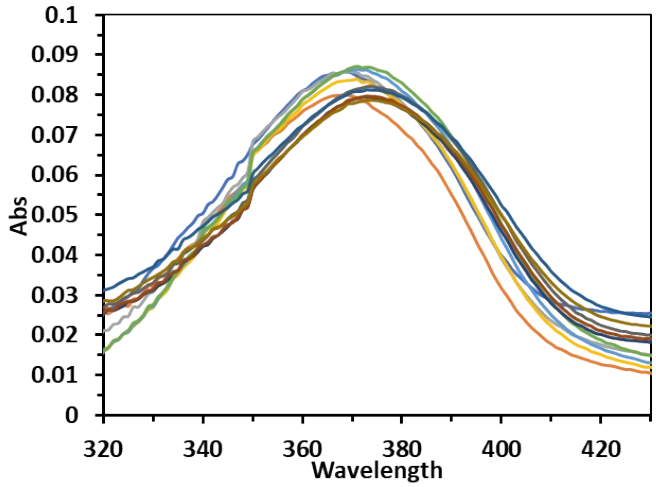

Figure S1g: The absorbance-based aggregation study of **NPG** (5 μM) in DMF and its aqueous binary mixtures at different volume fractions of water. Ex = 360 nm; Slit width: Ex = 5 nm and Em = 3 nm.

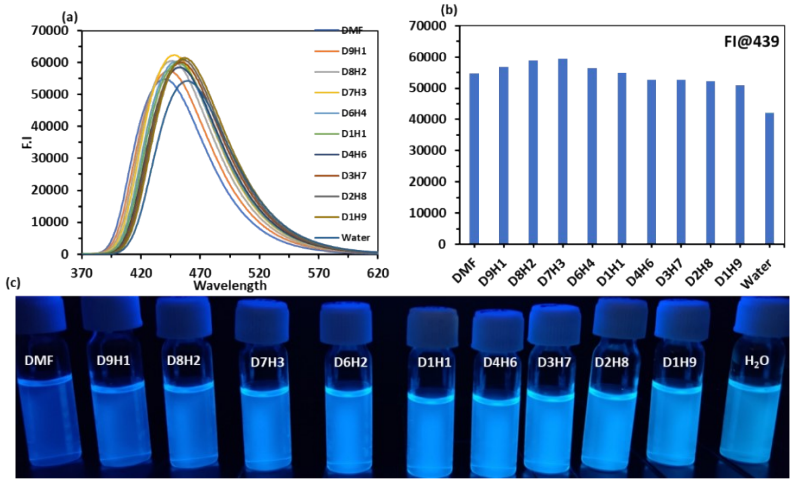

Figure S2. Fluorescence based aggregation study of **NPG** (5 μM) in DMF and its aqueous binary mixtures at different volume fractions of water. Ex = 360 nm; Slit width: Ex = 5 nm and Em = 3 nm.

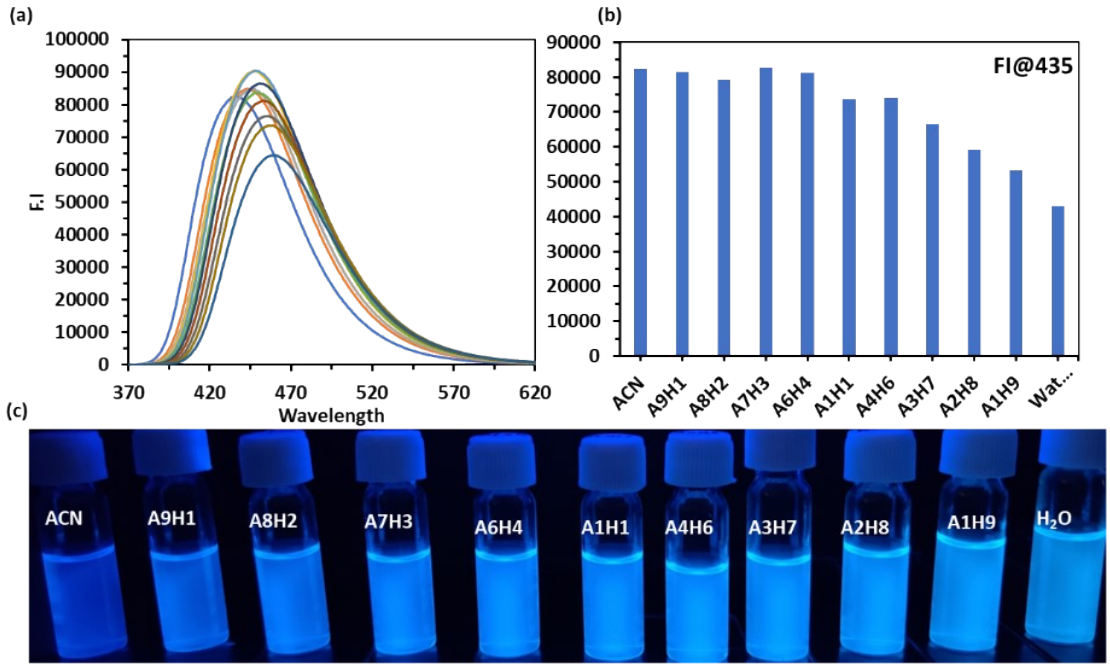

Figure S3. Fluorescence based aggregation study of **NPG** (5 μM) in CH_3CN and its aqueous binary mixtures at different volume fractions of water. Ex = 360 nm; Slit width: Ex = 5 nm and Em = 3 nm.

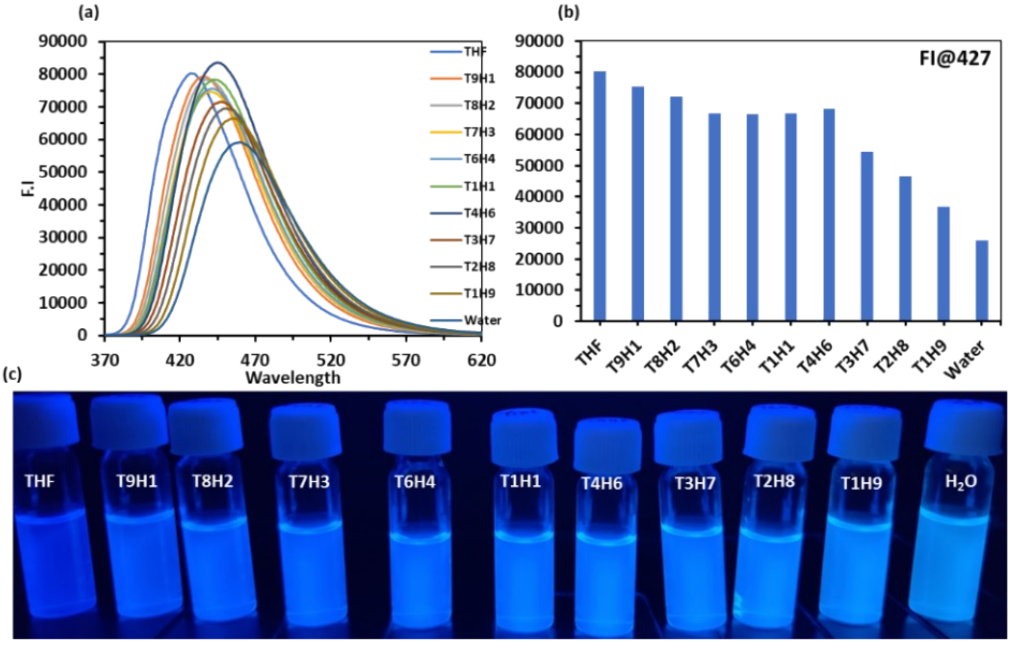

Figure S4. Fluorescence based aggregation study of **NPG** (5 μM) in THF and its aqueous binary mixtures at different volume fractions of water. Ex = 360 nm; Slit width: Ex = 5 nm and Em = 3 nm.

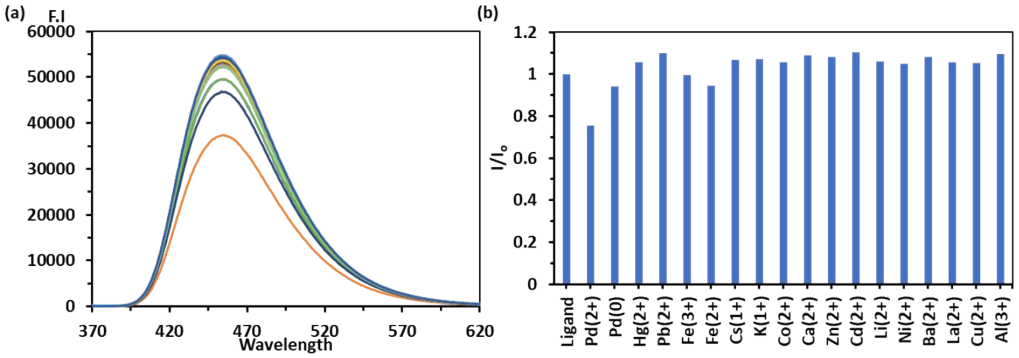

Figure S5. (a) Emission spectra and (b) bar graph of **NPG** upon addition of different metal ions in HEPES buffer-DMSO (1: 1 v/v, pH 7.2) solution, Ex = 360 nm; Slit widths: Ex = 5 nm and Em = 3 nm.

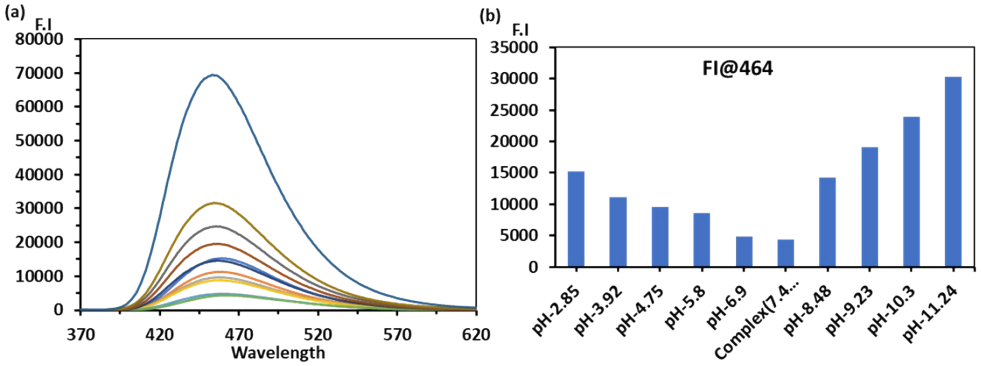

Figure S6. (a) Emission and (b) bar graph of **NPG**+Pd^{2+} complex recorded in DMSO: H_2O (1:1) solution at different pH values; Ex = 360 nm; Slit width: Ex = 5 nm and Em = 3 nm.

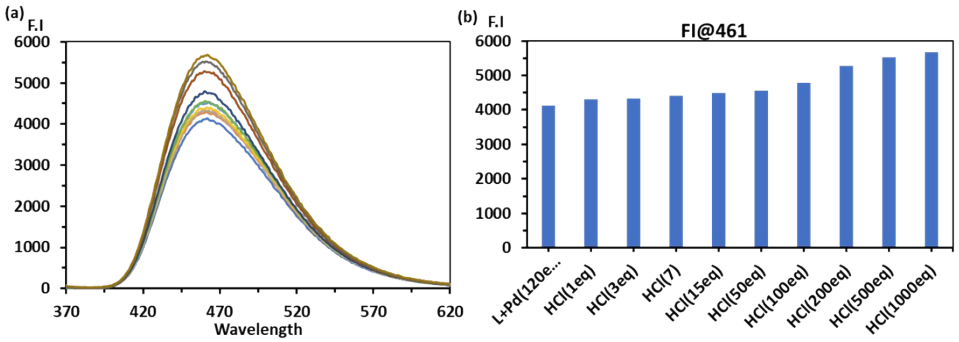

Figure S7. (a) Emission and (d) bar graph of **NPG**+Pd^{2+} complex recorded in DMSO: H_2O (1:1) solution on incremental addition of HCl; Ex = 360 nm; Slit width: Ex = 5 nm and Em = 3 nm.

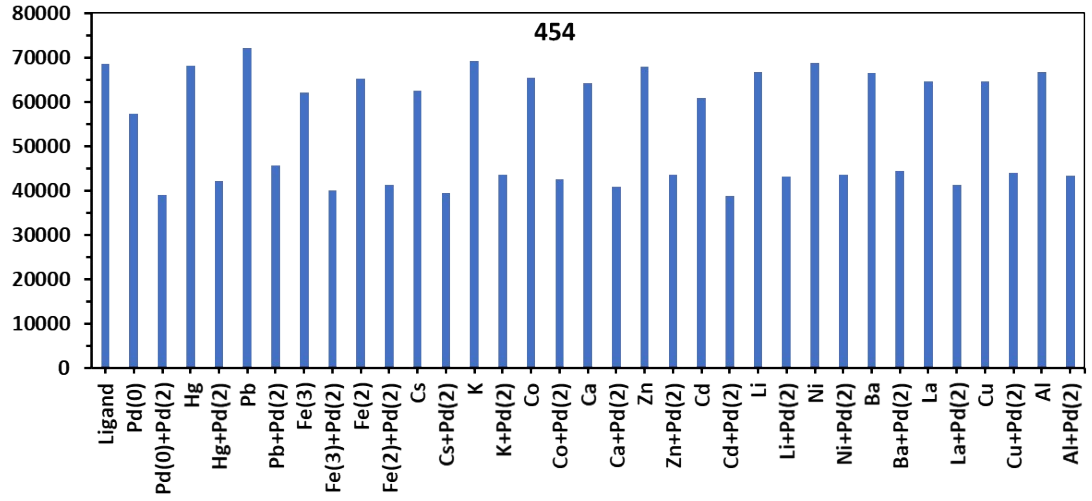

Figure S8. Fluorescence based interference study of **NPG** (5 μM) complex of Pd^{2+} with other metal ions in HEPES buffer–DMSO (1:1, pH 7.2), Ex = 360 nm; Slit widths: Ex = 5 nm and Em = 3 nm.

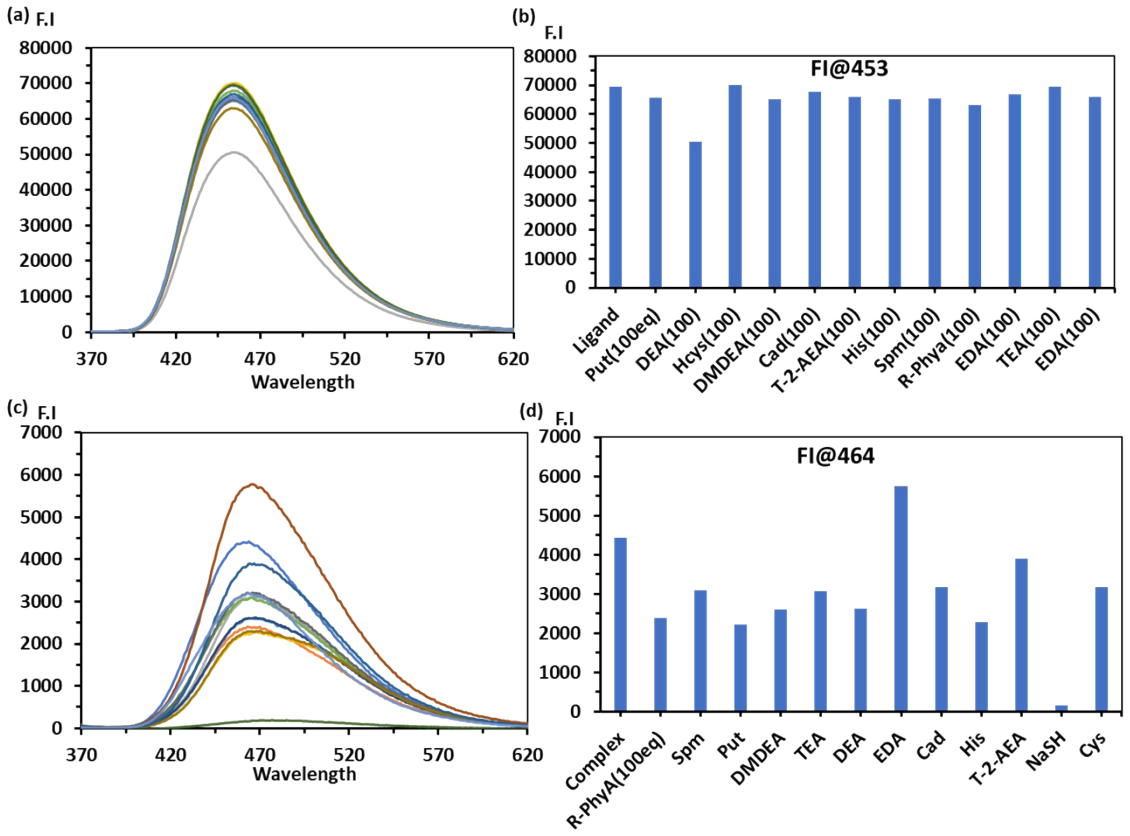

Figure S9. (a) Emission spectra and (b) bar graph of Fluorescence based amines (100 equiv.) study **NPG** (5 μM) in 50% HEPES buffer: DMSO solution; Ex = 360 nm; Slit width: Ex = 5 nm and Em = 3 nm; (c) Emission spectra and (d) bar graph of fluorescence-based amines (100 equiv.) study **NPG**+Pd^{2+} complex (5 μM) in 50% HEPES buffer: DMSO; Ex = 360 nm; Slit width: Ex = 5 nm and Em = 3 nm.

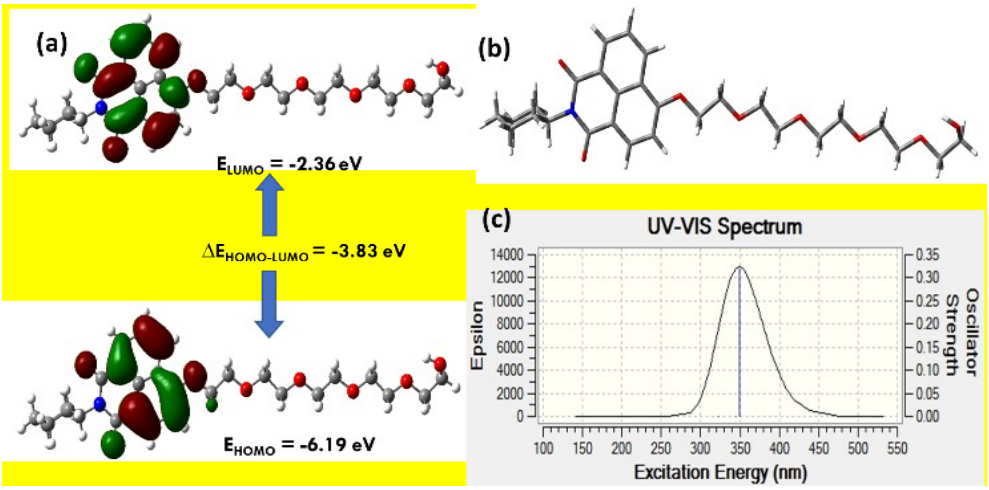

Figure S10. (a) The HOMO and LUMO; (b) energy optimized structure and (c) TD-DFT of **NPG** calculated with DFT using B3LYP/6-31G* basis sets.

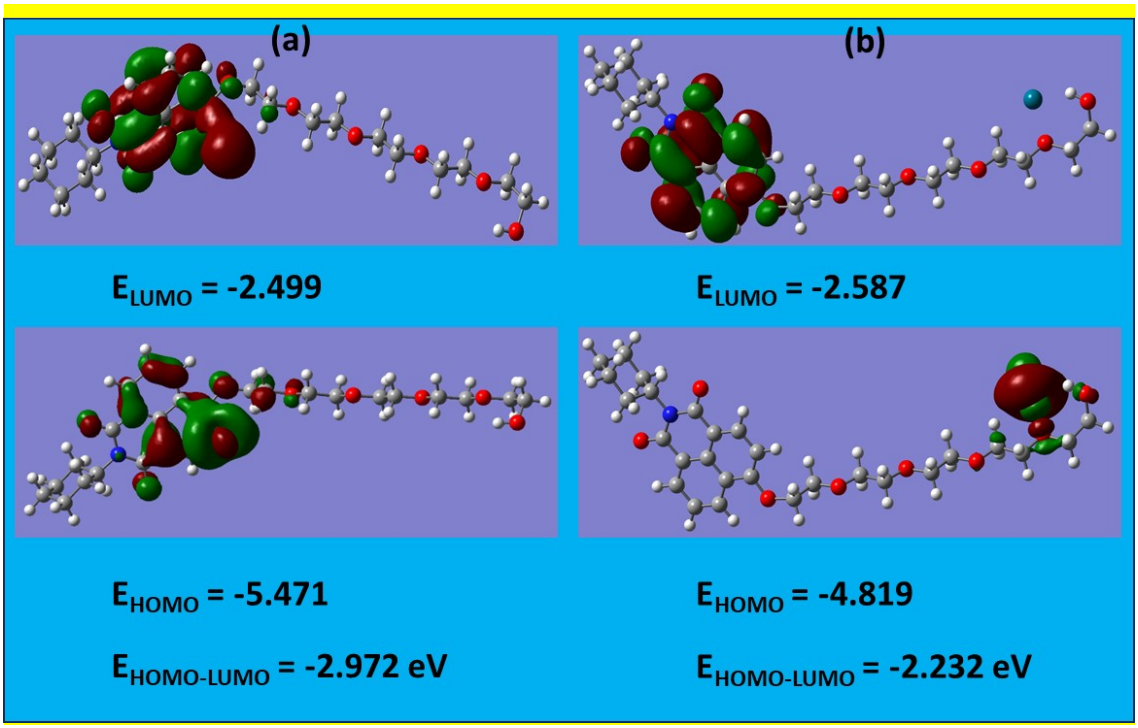

Figure S11: The HOMO and LUMO of **NPG-**Pd^{2+} complex calculated with DFT using B3LYP/6-31G* basis sets. The Pd^{2+} ions were placed (a) near the naphthalimide ring; (b) near the terminal oxygen atoms of glycol chain.

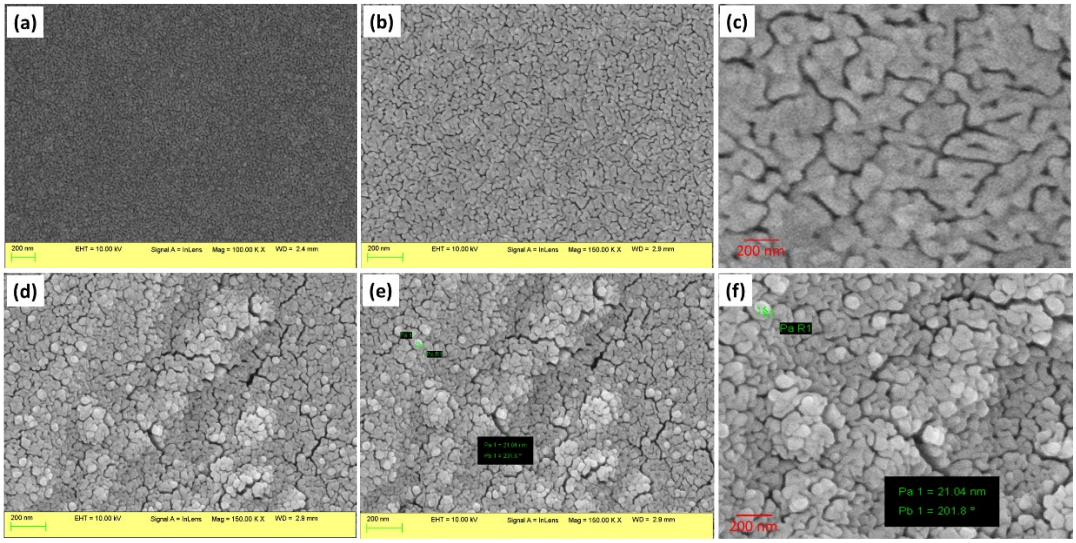

Figure S12. SEM images of (a-c) **NPG** and (d-f) **NPG**+Pd^{2+} complex recorded in HEPES buffer–DMSO (1:1, v/v, pH 7.2) solution.

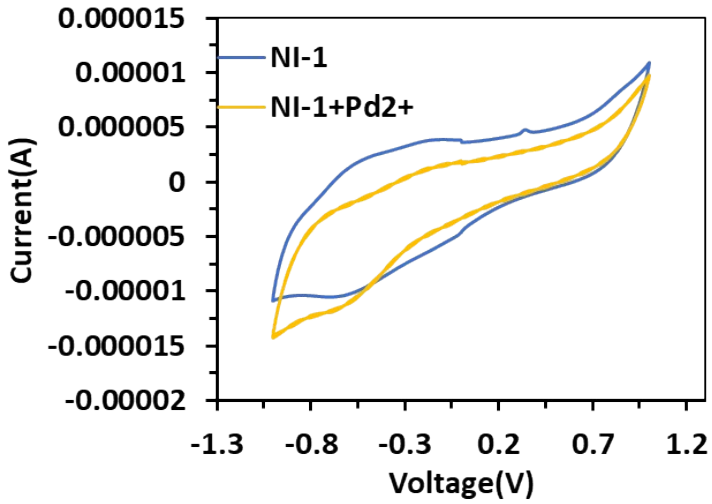

Figure S13. Cyclic voltametric (CV) data of **NPG** and **NPG**+Pd^{2+} complex recorded in HEPES buffer–DMSO (1:1, v/v, pH 7.2) solution.

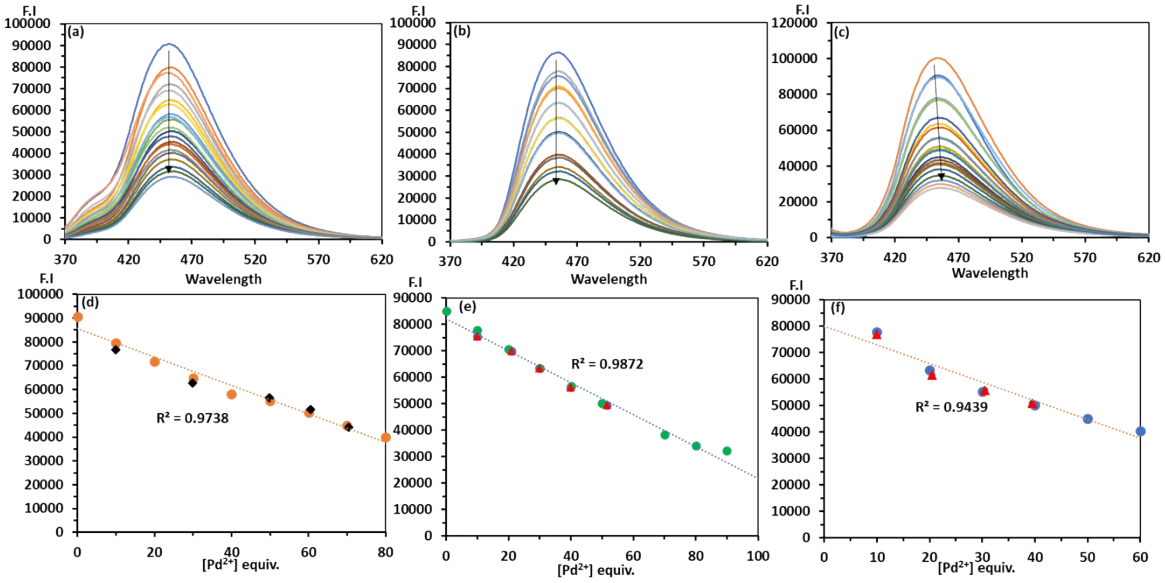

Figure S14: (a-c) Fluorescence spectra and (d-f) fluorescence profile of **NPG** after incremental addition of Pd^{2+} ions recorded in HEPES buffer-DMSO (1:1, v/v, pH 7.3), containing 10% tablet solution, 10% urine solution and 10% human blood serum, respectively.

Table S1: Comparison of literature reports for the detection of Pd^{2+} ions have been added in the supporting information.

System	Method	Analyte	Type of Sensor	Solvent system	λ_{max} (NIR)	Response Time	Detection limits	Applications	Reference
NPG	Fluorescence	Pd^{2+}	Chemosensor	DMSO-HEPES (1:1)	450 nm (FI)	Immediate response	72 nM (FI),	Live cell imaging, Quantification of Pd species in drug samples, anticounterfeiting, solid-state detection	Present Report
DNP	UV-Vis , Fluorescence	Pd^0, Pd^{2+}, TPP	Chemod -osimeter	ACN-HEPES (1:1)	**In NIR Region** A_{759nm}/A_{560nm} (Pd^0, Pd^{2+}), A_{698nm}/A_{560nm} (TPP)	30 minutes	190 nM (Pd^0), 283 nM (Pd^{2+}), & 349 nM for TPP	Live cell imaging, Solution, solid-TLC based detection of Pd &TPP in aqueous ACN (1:1)	ChemistrySelect, 2023, 8, e202300693
Acylhydrazone-based fluorescent sensor	Fluore scence	Pd^{2+}, $H_2PO_4^{2-}$	Chemosensor	DMF	**No NIR** 475 nm (FI)	-	2.03×10^{-8} M	Formation of heterogeneous catalyst for C-C coupling with reused for at least 5 times	Journal of Molecular Liquids 327 (2021) 114836

Rhodamine & Coumarin-rhodamine based (FRET) sensor	UV-Vis , Fluorescence	Pd^0, Pd^{2+}	Chemosensor	ACN-H_2O (1:1)	**No NIR** 570 nm (UV), I_{599}/I_{470} (FI)	60 min	Using FI 82 nM **(FPS) &** 70 Nm **(RPS)**	Live cell imaging	Talanta 210 (2020) 120634
Purine functionalized rhodamine B	UV–visible, Fluorescence	Pd^{2+}	Chemosensor	EtOH-Hepes (3:2)	**No NIR** 562 nm (UV), 584 nm (FI)	-	49.5 nM for Pd^{2+}	Test paper based Solid-state quantitative detection of Pd^{2+}	Inorganic Chemistry Communications 102 (2019) 233–239
Allyl carbonate substituted coumarin derivative	UV–visible, Fluorescence	Pd^0,	Chemod -osimeter	EtOH-PBS buffer (2 : 3)	**No NIR** 324 and 473 nm (UV), 560 nm (FI)	10 minutes	4.18 µM (FI)	Live cell imaging, studies in zebrafish	New J. Chem., 2019, 43, 548--551
Purine derivative based Schiff base **PTAID**	UV–vis and fluorescence	Pd^{2+}, Cu^{2+}	Chemosensor	DMSO-HEPES (3:2)	**No NIR** 375 nm (UV-Vis), 501 nm (FI)	3 min	0.63 µM for $Pd^{2+}$and 1.19 µM for Cu^{2+}	Solid- state detection of Pd^{2+}, Cu^{2+} on paper,	Inorganic Chemistry Communications 116 (2020) 107915
Imidazolium ionic liquid functionalized salicylaldehyde bis-Schiff-base	UV–vis and fluorescence	Pd^{2+}, Cu^{2+}	Chemod -osimeter	HAc–NaAc buffer for Pd^{2+}	**No NIR** A_{412nm}/A_{350nm}, 425 nm (for Pd^{2+}) and A_{412nm}/A_{350nm} (for Cu^{2+})	-	0.076 µM (Pd^{2+}), 0.080 µM (Cu^{2+})	solid-state TLC-strips based detection of Pd^{2+}, Determination of Pd^{2+} in real water	Spectrochimica Acta Part A: Molecular and Biomolecular Spectroscopy 237 (2020) 118365
Functionalized 3-(2,3,3-trimethyl-	UV–vis and Fluorescence	Pd^{2+}	Chemod	DMSO-PBS	**In NIR** Dec. in 300-	30 min	0.52 µM (FI)	Pd^{2+} in real water samples	Inorganic Chemistry

3H-inulinyl) propane **Cy202**			-osimeter	buffer solution (pH 7.40, 8:2, v/v)	500 nm & inc in 500-700 nm (UV) 689 nm (FI)				Communications 101 (2019) 135–141
Rhodamine derivative (**YG)**	Fluorescence	Pd^{2+}	Chemosensor	Ethanol-PBS (2:8)	**No NIR** 575 nm (FI)	-	0.39 µM (FI)	Live cell imaging of Pd^{2+} and ClO^- using L929 cells	Tetrahedron 75 (2019) 130570
Allyl carbonate **(C1) &** propargyl **(C2)** substituted coumarin-based probes	Fluorescence	Pd^0, Pd^{2+} N_2H_4	Chemod -osimeter	CH_3CN-PBS (1:3)	**No NIR** 509 nm (C1), I_{524nm}/I_{412nm} (C2) and 37 Nm for N_2H_4	2–3 min	33 nM (C1), 14 nM (C2) and 37 nM for N_2H_4	-	Sensors and Actuators B 256 (2018) 1107–1113